

Prediction of Unsteady Turbulent Flow over a Square Cylinder using Two-Equation Turbulence Models

2-방정식 난류모델을 이용한 정사각주 주위 비정상 난류 유동의 예측

Sangsan Lee*¹
이 상산

비유선형의 물체 주위의 유동은 정체유동, 경계층 박리 및 주기적 와열 생성 등의 복잡한 유동현상이 공존한다. 본 연구에서는 비교적 단순한 형상인 정사각주 주위의 비정상 난류 유동을 2-방정식 와점성 난류모델인 표준 $k-\epsilon$ 모델과 RNG $k-\epsilon$ 모델을 이용하여 예측할 수 있는지를 검증하였다. 정교하게 수행된 최근의 실험과 대와류모사(LES)의 결과를 검증을 위한 비교의 자료로 삼았다. 적절한 난류모델의 선정과 더불어 시간 정확도, 공간 정확도 및 대류항 처리법 등이 해석결과에 미치는 영향도 살펴보았다. 기존의 표준 $k-\epsilon$ 모델은 정체점 부근에서 난류 운동에너지를 과도하게 생성하는 근본적인 문제점 때문에 실험 및 LES의 결과를 제대로 예측할 수 없었다. 난류 운동에너지의 초과 예측에 따른 운동량의 과도한 혼합으로 인해, 항력계수 및 양력계수의 비정상성 뿐 아니라 평균 항력계수도 부정확하게 예측하였다. RNG $k-\epsilon$ 모델을 사용한 경우에는 정체점 주위 유동현상의 예측이 상당히 향상되어 항력계수 및 양력계수의 평균치, 진폭 및 비정상성의 주기 등을 정확하게 예측하는 것이 가능하였다. 그러나 이 경우에도 예측의 정확도가 시간 증분과 격자의 크기 및 대류항 처리법등에 영향을 받으며, 특별히 대류항 처리법에 상당히 민감하게 변하는 것을 알 수 있었다. 향상된 유동예측은 RNG $k-\epsilon$ 모델의 난류에너지 소산을 방정식의 개선된 항이 과도하게 생성된 난류에너지를 정체점 부근에서 제거하기 때문에 가능하다는 것을 알 수 있었다.

1. Introduction

Turbulent flow has apparently random fluctuations not only in space but also in time. And it is impracticable to accurately predict engineering turbulent flows even with the most advanced computers. Only turbulent flows at low Reynolds numbers may be predicted through direct numerical simulation (DNS), where the smallest meaningful length and time scales are resolved [1]. In highly turbulent flows, DNS requires impracticable huge computer resources in memory as well as in CPU hours. With the least turbulence modeling effort, namely a subgrid-scale (SGS) model, large-eddy simulation (LES) may be performed [1] for turbulent flows at high Reynolds numbers. Recently, active research [2,3,4] is under way in the field of SGS modeling, so that LES may be used as an engineering prediction tool with the advent of next-generation supercomputers with a Teraflops (10^{12} floating point operations per second) peak performance.

But the current computational capacity is not enough to support LES to be an engineering precaution tool, and the Reynolds-averaged, or Favre-averaged in compressible flows, Navier-Stokes equations are solved, where all the turbulence effects on the mean motion are taken into account by eddy viscosity models (EVM: for 0-, 1-, and 2-equation models) or by Reynolds stress models (RSM: for Reynolds stress transport models). Mixing-length model [5], a zero-equation model, is mostly widely used in flows, where turbulence effects are not too complex, such as in aerodynamic flows. Even though there has been some success with one-equation model [6], two-equation turbulence model is the most widely used in engineering predictions of turbulent flows, among them are $k-\epsilon$ models. More refined prediction may be conducted with RSM by solving Reynolds stress transport equations. Even though RSM, in general, gives better predictions, it is less popular since it tends to require far more computer resources compared to its $k-\epsilon$

¹ SERI/KIST (305-600, P.O. Box 1, Yuseong, Daejeon, Tel: 042-869-1834)

counterparts. Even with the popularity of the $k - \epsilon$ models, they have some fundamental defects: negligence of rotation, anisotropy, and non-equilibrium effects. Recent review on the conventional turbulence models is given in Bradshaw *et al.* [7].

Flows over blunt bodies are physically important in many engineering applications, such as automobiles, bridges, and buildings. Accurate prediction of such flows using turbulence models by computational fluid dynamics (CFD) is a very demanding issue. The main source of errors in the CFD predictions in such flows is the poor modeling of complex flow characteristics, especially of turbulence. To assess the limit of CFD in such applications, investigation has been made for canonical flows, such as flows over a circular cylinder [8] and over a square cylinder [9,10,11]. Recently, Myong [12] also recognized the importance of turbulent flow prediction around a stagnation point in blunt bodies to predict the flow around an automobile with accuracy: Actually most errors in the pressure distribution is found in the forward part rather than the rearward part of the automobile.

In the present paper, a systematic investigation is made to assess what are the important factors for the accurate prediction in an unsteady turbulent flow. In terms of physical modeling, two-equation turbulence models are tested, the standard $k - \epsilon$ model [13] and the RNG $k - \epsilon$ model [14]. The effects of numerical parameters--- spatial accuracy, temporal accuracy, convection scheme, are also investigated. In the following section, problem is formulated with governing equations, computational setup, and boundary conditions given. Experimental and simulation works quoted for comparison are also briefly explained. In section 3, the effects of physical models and numerical parameters on the prediction accuracy are described. In the final section, the required physical model and numerical setups are summarized.

2. Problem Formulation

Turbulent flow over a square cylinder is computed numerically as a canonical blunt body flow. Simulation is carried out in two dimensions, and three dimensionality of the mean flow is not accounted for. Recently, Lyn and Rodi [15] conducted a well-controlled wind tunnel experiment, which is used as a reference case. All the computational setups are aimed at simulating the experiment, and the computational results are compared with the experiment as far as the experimental measurement data are available. Some other turbulence quantities could not be measured, and LES simulation results [9] are used for comparison.

The experiment of Lyn and Rodi is conducted in a wind tunnel with 0.56m by 0.39m test section. The square cylinder is 0.04m by 0.04m (7% blockage ratio) with length of 0.39m, and the free stream wind speed is 0.535 m/sec with 2% turbulence intensity. Special attention is given to successfully suppress the mean flow three-dimensionality due to end effects. The upstream mean flow is modified by the cylinder presence less than 10% in $2.5D$ ($D=0.03m$) upstream of the blockage. The LES is conducted for the configuration of the experiment. The computational domain is $20D \times 14D \times 2D$ which are divided in to $104 \times 69 \times 10$ grid points in the streamwise, normal, and the cylinder axis direction, respectively. The usual computation takes about 60 CPU hours in the Fujitsu VP2600 supercomputer (5 Gflops peak performance) to get statistically converged unsteady turbulent flow patterns.

In the present study, the computational domain is set up two dimensionally. The nonuniformly distributed grid points used in the reference case are 85×55 in the streamwise and normal direction, respectively. For the coarse and the refined grid case, grid points of 65×50 and 120×75 are used respectively. Their detailed distributions near the wall are described later.

The governing equations solved are the conservation of mass and momentum, expressed as

$$\frac{\partial u_j}{\partial x_j} = 0$$

$$\frac{\partial u_i}{\partial t} + \frac{\partial u_j u_i}{\partial x_j} = -\frac{1}{\rho} \frac{\partial p}{\partial x_i} + \frac{\partial}{\partial x_j} \left((v + v_T) \left(\frac{\partial u_j}{\partial x_i} + \frac{\partial u_i}{\partial x_j} \right) \right),$$

where the repeated indices denote the summation over all directions. And the eddy viscosity v_T is evaluated by turbulence kinetic energy (k) and its dissipation rate (ϵ) as $v_T = c_\mu k^2 / \epsilon$, and k and ϵ are governed by the following transport equations.

$$\frac{\partial k}{\partial t} + \frac{\partial u_j k}{\partial x_j} = \frac{\partial}{\partial x_j} \left(\left(\nu + \frac{\nu_T}{\sigma_k} \right) \frac{\partial k}{\partial x_j} \right) + P_k - \varepsilon$$

$$\frac{\partial \varepsilon}{\partial t} + \frac{\partial u_j \varepsilon}{\partial x_j} = \frac{\partial}{\partial x_j} \left(\left(\nu + \frac{\nu_T}{\sigma_\varepsilon} \right) \frac{\partial \varepsilon}{\partial x_j} \right) + \frac{\varepsilon}{k} (C_{\varepsilon 1} P_k - C_{\varepsilon 2} \varepsilon) ,$$

where the production rate P_k is defined as

$$P_k = \nu_T \frac{\partial u_i}{\partial x_j} \left(\frac{\partial u_j}{\partial x_i} + \frac{\partial u_i}{\partial x_j} \right) ,$$

and the coefficients are chosen as follows in the standard [13] and the RNG $k - \varepsilon$ models [14]:

(1) the standard model:

$$c_\mu = 0.09, \sigma_k = 1.0, \sigma_\varepsilon = 1.3, C_{\varepsilon 1} = 1.44, C_{\varepsilon 2} = 1.92$$

(2) the RNG model:

$$c_\mu = 0.085, \sigma_k = 0.72, \sigma_\varepsilon = 0.72, C_{\varepsilon 2} = 1.68,$$

$$C_{\varepsilon 1} = 1.42 - \frac{\eta(1 - \eta / \eta_o)}{1 + \beta \eta^3}$$

where $\beta = 0.012$, $\eta_o = 4.38$ and $\eta = Sk / \varepsilon$ with $S = \sqrt{2S_{ij}S_{ij}}$ (S_{ij} is the strain rate tensor).

To simulate the experimental setup with minimal computational cost, symmetry boundary condition is imposed instead of no-slip wall. Effects of the symmetry boundary condition to the unsteady turbulent flow around the cylinder is found negligible [10,11]. Near the cylinder surface, wall function is used with the standard linear-log law-of-the-wall as the boundary condition. In most computations, the minimum grid spacing is kept between 10 to 20 wall units near the wall with proper stretching away from the cylinder. The governing equations are approximated through a finite-volume approach with all the flow variables evaluated at the cell center [16]. The convection term is treated by upwind, hybrid, and QUICK scheme [17] and all the other spatial derivatives are approximated by the second order central difference. Mass conservation is imposed by solving the pressure correction equation of SIMPLE type [18]. Temporal advancing is made by the backward Euler scheme and the normalized time step $U\Delta t / (\Delta x_i)_{\min}$ is taken as around 0.7, where U is the free stream velocity and $(\Delta x_i)_{\min}$ is the minimum grid spacing. The usual local CFL number exceeds 2 near the forward corner of the cylinder for the reference case.

3. Results and Discussion

In the following, numerical setup and the computational results from a reference case are described and compared with the experiments and the LES. And the results are justified by investigating the effects of temporal accuracy and grid refinement. The effects of turbulence model and convection scheme are described.

3.1 A Reference Simulation

The computation is carried out after the governing equations are normalized by the reference velocity and length scale with the free stream velocity and the cylinder side length. And the flow Reynolds number ($Re = UD / \nu$) is 22,000. The computation is initialized with a uniform free stream velocity field except the zone occupied by the cylinder. The important numerical parameters of the reference simulation and of the simulations to be discussed later are listed in Table 1. The dimensionless grid spacing adjacent to the wall, $(\Delta x_i)^+ = (\tau_w / \rho)^{1/2} \Delta x_i / \nu$, is ranging from 10 to 40 with the average of about 20.

Instantaneous vorticity and pressure fields at different time instants are shown in Fig. 1, where flow unsteadiness and asymmetry are clearly noticed. Since unsteady regular vortex shedding is the main feature of the flow, the drag (c_D) and lift (c_L) coefficients represent the unsteady behavior of integrated flow field around the cylinder. In the evaluation of the drag and lift forces, viscous stress is also included in addition to pressure. However, the viscous stress contributes to the total force less than a percent of the total. The evolution of the drag and lift coefficients from

Table 1. Numerical parameters and results of the conducted simulations

| case | Δt^* | Δx^* | Convection | Turbulence | c_D | c_L | St |
|---------|--------------|--------------|-------------------------|------------|------------------|------------|-------------------|
| REF | 0.65 | 0.035 | QUICK | RNG | 2.12 ± 0.23 | ± 2.08 | 0.133 ± 0.003 |
| 2DT | 1.30 | 0.035 | QUICK | RNG | 2.30 ± 0.18 | ± 2.07 | 0.135 ± 0.008 |
| 5DT | 3.25 | 0.035 | QUICK | RNG | 2.23 ± 0.14 | ± 2.01 | 0.138 ± 0.009 |
| 10DT | 6.50 | 0.035 | QUICK | RNG | 2.15 ± 0.13 | ± 1.82 | # |
| DXC | 0.68 | 0.074 | QUICK | RNG | 1.62 ± 0.02 | ± 0.40 | 0.141 ± 0.003 |
| DXF | 1.67 | 0.012% | QUICK | RNG | 2.37 ± 0.44 | ± 2.04 | 0.130 ± 0.003 |
| THR | 0.65 | 0.035 | Hybrid | RNG | 1.90 ± 0.05 | ± 0.77 | 0.134 ± 0.009 |
| TUR | 0.65 | 0.035 | Upwind | RNG | 1.83 ± 0.02 | ± 0.55 | 0.130 ± 0.011 |
| TQS | 0.65 | 0.035 | QUICK | Standard | 1.75 ± 0.004 | ± 0.56 | 0.138 ± 0.013 |
| TUS | 0.65 | 0.035 | Upwind | Standard | 1.71 ± 0.016 | ± 0.32 | 0.125 ± 0.013 |
| Exp[15] | | | | | 2.14 ± 0.09 | | 0.134 |
| LES[9] | 0.004 | 0.050 | 2 nd Central | SGS | 2.09 ± 0.13 | ± 1.60 | 0.132 |

Definition: $\Delta t^* = U \Delta t / (\Delta x_i)_{\min}$, $\Delta x^* = (\Delta x_i)_{\min} / D$,

#: Accurate single frequency evaluation is impossible.

?: Since $(\Delta x_i)^+ < 10$ in most regions adjacent to the wall, BC for ε is locally inconsistent.

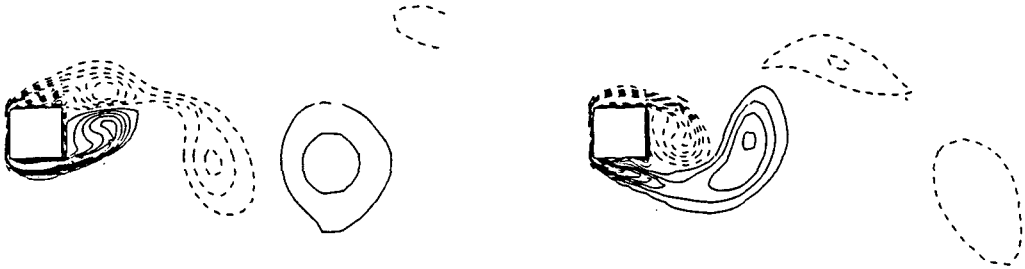


Fig. 1 Instantaneous vorticity fields at the opposite phase of the oscillation: solid lines denote for positive, and dashed lines for negative vorticity ($\Delta\omega = 1.0$).

the simulation are shown in Fig. 2. It shows an initial transient lasting around 100 time units followed by regular oscillations with a low frequency modulation. Time history of the lift coefficient after the initial transient (time between 120 to 260) is taken and the dominant frequency is estimated by FFT with proper windowing [19] to remove the effects of signal non-periodicity. The estimated Strouhal number ($St = fD / U$) is 0.133 with an uncertainty limit of 0.003. Other statistics like the mean and peak force coefficients are also evaluated using the signal: The mean and variation amplitude of c_D are 2.12 and 0.23, the variation amplitude of c_L is 2.08. The statistics of force coefficients for the computations conducted in this study are also shown in Table 1 along with those from the experiment [15] and from the computations [9] for comparison. First of all, the LES results compare very well with the experiment, which validates the quality of the simulation. Therefore, the data not available from the experiment--- the amplitude of c_D and c_L variation, is taken from the LES as a reference to compare the present computation results. The statistical results of the reference simulation compare well with the experiments and also with the LES results, especially in the average drag coefficient and the Strouhal number. Differences in the unsteady part of force coefficients may be due to inherent three-dimensionality of turbulence which is not accounted for in the current computation. Hence, the deterministic unsteady forces in the present work tend to be higher than the experiment and the LES results. This is analogous to the observation made by Vickery [20]: A cylinder in a fully turbulent free stream feels smaller unsteady forces than the one in a smooth stream.

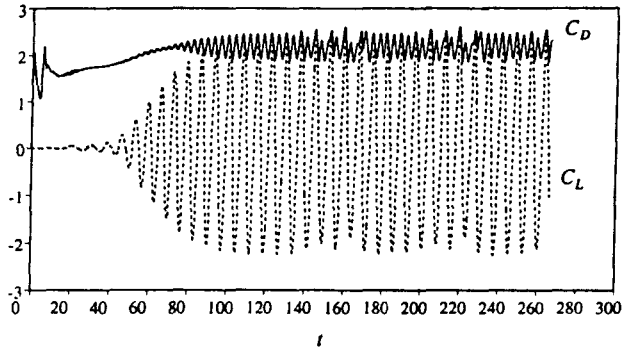


Fig. 2 Evolution of force coefficients in the reference simulation (case REF).

In order to investigate the effect of the temporal accuracy, time step has been increased progressively from the reference time step ($\Delta t^* = 0.65$) to $\Delta t^* = 6.5$ (case 10DT), with the same grid. Since the unconditionally stable Euler implicit scheme is used for time advancing, numerical instability does not occur. Time steps taken for one-period of vortex shedding is decreased from around 700 (case REF) to 70 (case 10DT). The force coefficients are not very sensitive to the time step used upto $\Delta t^* = 3.25$ (case 5DT). However, the reference time step has been used for other simulations to accurately evaluate the unsteady loading frequencies.

The effect of the mesh resolution is investigated by coarsening (DXC) and refining (case DXF) the meshes near wall more than by a factor of 2. The reference resolution is found to be enough for the present study, since we noticed little difference from the reference case to the refined case considering local inconsistency of wall function approach in case DXF with $(\Delta x_i)_{\min}^+ < 10$. Since the use of a coarser grid may affect the computation accuracy, the reference resolution is used for other simulations.

It takes about 1 CPU sec for the reference simulation to advance one time step in CRAY Y-MP C90 with the absolute cell mass flux residual sum to be less than 10^{-4} of the inflow mass flux at the end of each time step.

3.2 Effects of Convection Schemes

With the lower order convection scheme like hybrid or upwind schemes, unsteady force coefficients are underestimated. Force coefficients predicted are the largest for the QUICK (cases REF, TQS), then for the hybrid (case THR), and the smallest for the upwind scheme (cases TUR, TUS) for a given turbulence model. In general, more dissipative scheme gives smaller force coefficients. This is consistent with the observation made by Vickery [20]: Unsteady force coefficients are smaller for turbulent flows than for laminar flows by about 50%. In other words, the added numerical dissipation from the lower order convection schemes contribute the flows to behave closer to more turbulent flows, hence reduces the unsteady forces.

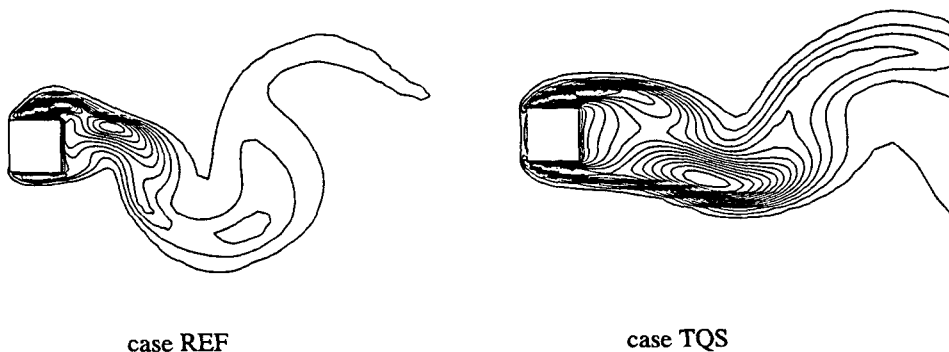


Fig. 3 Instantaneous TKE fields from case REF (RNG) and from case TQS (Standard) at the same phase of the oscillation ($\Delta k = 0.01$)

3.3 Effects of Turbulence Models

There is a fundamental defect of the standard $k-\varepsilon$ model near the stagnation point, where turbulence kinetic energy (TKE) is produced significantly without any mechanism active in the region to remove or transport the excessively produced TKE. This defect leads to enhanced spurious turbulence motion in the forward stagnation point in the present simulation (cases TQS, TUS), that the flow is overmixed to give smaller regular unsteady forcing on the cylinder.

With the use of the RNG $k-\varepsilon$ model, which has similar structures $k-\varepsilon$ equations with modifications of model constants: especially of $C_{\varepsilon 1}$ depending on the relative importance of the local strain rate to the turbulence time scale. In the vicinity of the stagnation region, this modified term enhanced the generation of dissipation rate, which makes enhanced rate of TKE dissipation. This enhanced dissipation rate prevent the augmentation of TKE in the region, which makes the force coefficients predicted by the computation (case REF) close to the experiment and the LES results. This can be clearly noticed in instantaneous TKE fields from case REF (with the RNG model) and from case TQS (with the standard model) shown in Fig. 3.

4. Summary and Conclusion

A conventional two-equation turbulence model (the RNG $k-\varepsilon$ model) is found to successfully reproduce the unsteady turbulent flows over the square cylinder without piling up TKE near the forward stagnation point, which has been regarded as a fundamental defect of the standard $k-\varepsilon$ model. For the proper prediction, time accuracy, spatial accuracy and high-order convection scheme are also needed in addition. The prediction results are quite sensitive to the spatial resolution, the choice of convection schemes, and turbulence models adopted. The difference persisting even in the most refined simulation is thought to be a fundamental defect of two-dimensional Reynolds-averaged turbulence models, such as eddy viscosity models (EVM) and Reynolds-stress models (RSM), which unfortunately does not seem to be easily removed and requires serious modeling efforts in the near future.

Reference

- [1] Rogallo, R.S. and Moin, P., (1984) "Numerical Simulation of Turbulent Flows," in *Annual Review of Fluid Mechanics*, Van Dyke et al. (Ed.), Academic Press, CA, p.99.
- [2] Germano, M., Piomelli, U., Moin, P., and Cabot, W., (1991), *Phys. Fluids A*, Vol. 3, p. 1760.
- [3] Moin, P., Squires, K., Cabot, W., and Lee, S., (1991), *Phys. Fluids A*, Vol. 3, p. 2746.
- [4] Ghosal, S., Lund, T., Moin, P., and Akselvoll, K., (1995), *J. Fluid Mech.*, Vol. 286, p. 229.
- [5] Baldwin, B.S. and Lomax, H., (1978), "Thin-Layer Approximation and Algebraic Model for Separated Turbulent Flows," *AIAA Paper No. 78-0257*.
- [6] Spalart, P.R. and Allmaras, S.R., (1992), "A One-Equation Turbulence Model for Aerodynamic Flows," *AIAA Paper No. 92-0439*.
- [7] Bradshaw, P., Launder, B.E., and Lumley, J.L., (1994), "Collaborative Testing of Turbulence Models," in *Advances in Computational Methods in Fluid Mechanics*, Ghia et al. (Ed.), ASME.
- [8] Mittal, R. and Balachandar, S., (1995), *Phys. Fluids*, Vol. 7, p.1841.
- [9] Murakami, S. and Mochida, A., (1995), *J. Wind Eng. Ind. Aerodynamics*, Vol. 54, p. 191.
- [10] Franke, R. and Rodi, W., (1991), "Calculation of Vortex Shedding past a Square Cylinder with Various Turbulence Models," *8th Symposium on Turbulent Shear Flow*, Munich.
- [11] Kato, M. and Launder, B.E., (1993), "The Modelling of Turbulent Flow around Stationary and Vibrating Square Cylinders," *9th Symposium on Turbulence Shear Flow*, Kyoto.
- [12] Myong, H.K., (1995), Personal Communication.
- [13] Launder, B.E. and Spalding, D.B., (1974), *Comp. Meth. Appl. Mech. Eng.*, Vol. 3, p. 269.
- [14] Yakhot, V., Orszag, S.A., Thangam, S., Gatski, T.B., and Speziale, C.G., (1992), *Phys. Fluids A*, Vol. 7, p.1510.
- [15] Lyn, D.A. and Rodi, W., (1994), *J. Fluid Mech.*, Vol. 267, p. 353.
- [16] Rhie, C.M. and Chow, W.L., (1983), *AIAA J.*, Vol. 21, p. 1527.
- [17] Leonard, B.P., (1979), *Comp. Meth. Appl. Mech. Eng.*, Vol. 19, p. 59.
- [18] Patankar, (1980), *Numerical Heat and Mass Transfer*, p.126, McGraw Hill, New York.
- [19] Press et al., (1986), *Numerical Recipes*, p. 423, Cambridge, New York.
- [20] Vickery, B.J., (1966), *J. Fluid Mech.*, Vol. 25, p.481.